Aluminium oxide barrier films on polymeric web and their conversion for packaging applications

C. F. Struller[a, b], P. J. Kelly[a], N. J. Copeland[b], V. Tobin[c], H. E. Assender[c], C. W. Holliday[d], S. J. Read[d]

[a]Surface Engineering Group, Manchester Metropolitan University, Manchester, M1 5GD, UK

[b]Bobst Manchester Ltd., Pilsworth Road, Heywood, Lancashire OL10 2TL, UK

[c]Department of Materials, University of Oxford, Begbroke Science Park, Oxford OX5 1PF, UK

[d]Innovia Films Ltd., Lowther R&D Building, West Road, Wigton, Cumbria, CA7 9XX, UK

ABSTRACT

In recent years, inorganic transparent barrier layers such as aluminium oxide or silicon oxide deposited onto polymer films have emerged as an attractive alternative to polymer based transparent barrier layers for flexible food packaging materials. For this application, barrier properties against water vapour and oxygen are critical. Aluminium oxide coatings can provide good barrier levels at thicknesses in the nanometre range compared to several micrometres for polymer-based barrier layer. These ceramic barrier coatings are now being produced on a large scale using industrial high speed vacuum deposition techniques, here, reactive evaporation on a 'boat-type' roll-to-roll metalliser. For the thin barrier layer to be useful in its final packaging application, it needs to be protected. This can be either via lamination or via an additional top coat. This study reports on acrylate topcoats, but also undercoats on aluminium oxide coated biaxially oriented polypropylene films. The effect of the acrylate layer on barrier levels and surface topography and roughness was investigated. The acrylate was found to smooth the substrate surface and improve barrier properties. Furthermore, the activation energy for water vapour and oxygen permeation was determined

in order to investigate barrier mechanisms. The oxide coated film was, additionally, converted via adhesive lamination, which also provided improvement in barrier levels.

Keywords: Aluminium oxide, BOPP, barrier coatings, reactive evaporation, lamination, acrylate coatings

1. Introduction

Transparent barrier films have been attracting increasing interest in recent years. Applications range from moderate barrier levels required for food packaging to very high barrier levels for encapsulating electronic devices. With the transparent barrier flexible packaging market growing worldwide at a rate of 10 to 15 % per year [1], the use of vacuum deposition techniques to produce transparent barrier layers such as aluminium oxide (AlO_x) or silicon oxide has become a favourable and powerful tool. For food packaging, this market is traditionally dominated by ethylene vinyl alcohol copolymer co-extruded barrier layer films and polyvinylidene chloride coated films [2]. However, vacuum-deposited barrier coatings only require a small fraction of the thickness of these barrier layers, i.e. their thickness is three orders of magnitude smaller, whilst still producing comparable barrier properties. The standard aluminium metallisation process, usually carried out in a roll-to-roll coater, can be modified by the injection of oxygen into the aluminium vapour in order to deposit a transparent aluminium oxide barrier layer; a process that has been developed over the last few decades [3-7]. The use of such large scale and high speed coating equipment can potentially provide vast economic and environmental benefits, which is of great importance for the low cost food packaging market where profit margins generally are small. Considering the low profit margins within the packaging market, the associated cost of the base substrate also plays an important role. On this point, biaxially oriented polypropylene (BOPP) base film still remains at a lower cost level than polyethylene terephthalate (PET) film, which causes it

to be the material of choice regarding commodity clear barrier films. Nevertheless, whilst PET films coated with reactively evaporated AlO_x give reliable barrier properties against water and oxygen, BOPP films have proven to be a more difficult substrate material. Here, the barrier levels strongly depend on the film surface characteristics and the resulting growth conditions for the AlO_x layer, as discussed in more detail in our earlier paper [7]. After coating with the thin barrier layer there is, though, a further conversion step required in order to obtain the final packaging structure. This is either achieved by laminating the vacuum coated films (adhesive lamination, extrusion lamination) or via application of an additional polymer coating on top of the inorganic layer, both serving the purpose of protecting the thin barrier layer during its final packaging application. Hence, it is essential that barrier loss upon conversion due to damage of the coating is avoided. In the course of this investigation, the effects of adhesive lamination as well as acrylate coatings on AlO_x coated polymer film was examined.

2. Experimental details

2.1. Substrate, coating and conversion processes

The film used in this study was a 20 µm thick three layer coextruded biaxially oriented polypropylene film with a homopolymer core and either a co- or terpolymer skin layer on each side. The film was also corona treated in-house by the film manufacturer. The corona treated side was coated with a 10 nm thin AlO_x layer via reactive thermal evaporation on an industrial roll-to-roll metalliser using a Bobst Manchester (formerly General Vacuum Equipment) General K4000 vacuum metalliser. This vacuum coater has a source consisting of resistively heated evaporation boats onto which aluminium wire is continuously fed. Oxygen is introduced into the aluminium vapour cloud to produce a transparent aluminium oxide coating and an optical monitoring beam and closed loop control system is used to

achieve consistent optical properties of the coated film across the web width and length. The pressure during aluminium oxide deposition is of the order of 0.05 Pa. AlO_x layers were deposited onto rolls of film (for acrylate top coats and lamination) and A4 samples mounted onto a carrier web (for acrylate undercoats). In the development work carried out, all coated film samples exhibit a transparency between 90 to 92 % visible light transmission, which is approximately equivalent to the light transmission of the uncoated BOPP substrate used. The transparency level is also maintained during the subsequent conversion processes of acrylate topcoating and lamination.

The acrylate deposition was achieved via flash evaporation of a monomer liquid in vacuum. These monomers condense as a liquid film on the substrate surface and are subsequently cured using electron beam radiation (with a current of 400 mA) to obtain a cross-linked layer. Acrylate deposition was carried out on a system licensed by Sigma Technologies International Inc. (USA). Tripropylene glycol diacrylate was chosen as a monomer and an acrylate thickness of 0.75 µm was deposited. Acrylate layers were coated onto A4 samples as undercoats and topcoats prior and after AlO_x deposition as an off-line process.

Lamination of the AlOx coated film was performed on an industrial laminator (Bobst Rotomec CL850) via solvent-based adhesive lamination. A high performance two component polyurethane adhesive was used and the AlO_x coated BOPP was laminated against another plain 20 µm BOPP film.

2.2. Analytical methods

Oxygen and water vapour transmission rates (OTR/WVTR) were determined in compliance with ASTM F 1927 and ASTM F 1249/ISO 15106-3 using a Mocon Oxtran 2/20 and Systech Illinois 8001 for oxygen permeation and a Mocon Permatran-W 3/33 and Systech Illinois 7001

for water vapour permeation. Test conditions for OTR were 23 °C and 50 % relative humidity (RH), whilst WVTR is stated for 37.8 °C and a gradient of 90 % RH. During WVTR measurement of coated samples, the coated side was always facing the 0 % RH. For the determination of the apparent activation energy of oxygen/moisture permeation, barrier measurements were carried out at 4 different temperatures (20 °C, 30 °C, 40 °C in addition to the respective temperature for a standard measurement).

A Veeco DI CP II atomic force microscope (AFM) in tapping mode was used to acquire roughness data and topography images. All images were corrected by first order line-wise levelling. Root mean square (RMS) values were calculated from 5 x 5 μm^2 size scans.

3. Results and discussion

3.1. Acrylate coated films

3.1.1 Barrier performance

The barrier performance of AlO_x coated BOPP with and without the application of acrylate top- and undercoats is summarised in *Table I*. Additionally, the barrier properties of the plain BOPP film and the acrylate coated BOPP film prior to AlO_x deposition are listed. As can be seen, the OTR of the plain film can be significantly reduced by the application of the inorganic AlO_x layer. Nevertheless, the improvement of WVTR is only marginal. These differences have been attributed to the film surface properties affecting coating nucleation and growth and thus the final structure of the thin AlO_x barrier layer [7, 8]. Furthermore, the use of an acrylate undercoat prior to AlO_x deposition can additionally enhance the oxygen as well as water barrier, though the acrylate on its own only slightly improves the plain film OTR and leaves the WVTR unchanged. This has also been reported by other research groups for AlO_x layers on polypropylene [9] and polyethylene terephthalate [10-13] and is assigned

to a variety of changes the acrylate confers to the polymer film. Acrylate layers have the capability to smoothen the substrate surface, eliminate surface features and thus decouple its defects from the subsequently deposited inorganic barrier layer [10, 12-15]. Furthermore, the barrier properties of the acrylate itself, which has a better oxygen barrier than BOPP [16], play a role, as this can affect and reduce the concentration gradient of the permeating substance in the polymer layer adjacent to the defect [17, 18]. Finally, the acrylate represents a change of surface chemistry which may offer more nucleation sites to the depositing inorganic coating thus resulting in a denser coating structure [9, 12]. The improvement seen when applying an acrylate topcoat, especially the significant enhancement of WVTR to less than 1 g/(m² d), could ~~can~~ be attributed to the protection of the barrier layer by the topcoat from damage during winding and handling, which is generally argued to be the reason for the barrier improvement [9, 10]. However, it is possible that infiltration of the acrylate into the defects of the AlO_x layer ('pore-filling') could lead to a reduction of the permeation coefficient within the defects from that of air to that of the acrylate [19]. A reduction in permeation has previously been reported for a post-winding laminated barrier film [20], and, more recently, a post-production chemical vapour deposition layer has also been reported to fill defects [21]. In our case, the samples were rewound in vacuum after AlO_x deposition as well as being handled prior to depositing the topcoat. Subsequently an acrylate coat was applied. So in our experiments, we were able to test whether the acrylate top-coat gave an inherent improvement in barrier due to pore-filling, rather than acting as a protection layer during winding and handling. Once again, the barrier properties of the acrylate should be mentioned here. Acrylate has a slightly better oxygen barrier than BOPP, nevertheless, it does not enhance the moisture barrier of BOPP (see *Table I*), i.e. its water vapour barrier is inferior. Hence, we conclude that to some degree the oxygen barrier improvement seen by the application of the topcoat may also be caused by the better oxygen barrier of the acrylate (and

therefore the resulting lower concentration gradient in the direct vicinity of defects). For the water barrier improvement seen we assume, though, that the pore-filling plays a major role.

3.1.2 Apparent activation energy

To further investigate the permeation mechanisms of oxygen and moisture through AlO_x coated and AlO_x/acrylate topcoated films, the activated rate theory was applied in order to calculate apparent activation energies of permeation [22-24]. The Arrhenius plots of this investigation and the activation energies obtained are summarised in *Fig. 1* and *Table II*, respectively. As can be seen, the activation energy of oxygen permeation remains largely unchanged by the application of the AlO_x layer as well as the acrylate topcoat, which indicates a macro-defect dominated permeation of oxygen through the coated film with the permeation through the BOPP polymer being the rate limiting step [25]. Furthermore, the activation energies obtained for oxygen are in agreement with values given in the literature [25-27]. For water vapour the AlO_x layer apparently slightly decreases the activation energy, whilst the application of the acrylate topcoat results in an increase back to the level of plain BOPP. It is, however, assumed that this change is not significant given the relatively small number of samples tested; in this case two (compare also the high standard deviations of activation energies obtained by Tropsha and Harvey [22]). The lack of significant change in activation energy is attributed to a macro-defect driven mechanism, as stated previously for oxygen permeation. This means that the vast majority of the permeating molecules passes through defects of the size of a few nanometres to several micrometres, whilst the rest of the coating can be assumed to be virtually impermeable. Consequently, the AlO_x layer primarily acts as a hurdle containing macroscopic defects, which the permeating molecules have to negotiate in order to enter/leave the polymer. There are, however, also a few cases published where despite the unchanged activation energy additional investigations suggested a chemical

interaction rather than a defect dominated permeation [22, 28]. The activation energy values for water vapour permeation through uncoated BOPP fall within the broad range of values reported in literature (Deng et al. [25] 64.6 ± 2.0 kJ/mol, Tropsha and Harvey [22] 38.9 ± 2.1 kJ/mol).

3.1.3 Surface topography

The surface topographies of the uncoated and acrylate undercoated films were additionally investigated. Differential interference contrast light microscopy (no images shown) revealed major changes induced by the acrylate with smaller filler particles being masked by the acrylate layer as well as the typical BOPP film texture ('orange-peel') being eliminated, which is in agreement with results published by other researchers [10, 14, 29]. AFM investigation of the uncoated and acrylate coated BOPP revealed a substantial decline of surface roughness with RMS values decreasing from 4.1 ± 0.3 nm to 1.1 ± 0.1 nm by the application of the acrylate layer, accompanied by a considerable change in surface structure, as can be seen in *Fig. 2*. The acrylate RMS roughness compares well with a range of 0.8 to 1.5 nm as stated by Affinito et al. [11]. This smoother surface could reduce the number of defects in the subsequently deposited AlO_x layer, and thus account for the improved barrier of the films with an acrylate undercoat, as reported in *Table I*.

3.2. Lamination

For the industrial scale lamination the AlO_x coated BOPP film was combined with an uncoated 20 µm BOPP film using a two component polyurethane adhesive. Thus, the thin AlO_x barrier layer is embedded between and protected by the BOPP films and is adjacent to the adhesive layer. As can be seen from the barrier performance pre and post lamination stated in *Table III*, the OTR could be significantly decreased, whilst WVTR was

approximately halved. The latter could be attributed to the doubling of the film thickness by adding another 20 µm thick BOPP film. The improvement of OTR is predominantly assigned to the barrier properties of the adhesive, which has a lower oxygen permeability compared to BOPP. This results in a reduction of the concentration gradient in the adhesive layer adjacent to the defects and therefore improves the overall oxygen barrier of the laminated structure containing the AlO_x barrier layer [30]. Furthermore, the infiltration of the adhesive into defects in the AlO_x layer, as discussed for the acrylate topcoat, has also been suggested by other researchers [31] to play an important role for the barrier improvement obtained by the adhesive lamination of vacuum coated polymer films.

4. Summary and conclusions

Acrylate top- and undercoats as well as adhesive lamination can significantly enhance the barrier performance of reactively evaporated AlO_x barrier layers on BOPP film. The change of surface chemistry and the smoothing of the BOPP film surface induced by the acrylate undercoat are thought to be of major importance for this barrier enhancement. During topcoating and presumably also lamination, the infiltration of the acrylate and adhesive into defects of the inorganic AlO_x layer, such as cracks, pinholes or pores, and the better oxygen barrier properties of the acrylate/adhesive can account for the obtained improvement of barrier levels. The investigation of apparent activation energy revealed a macro-defect driven permeation process through the AlO_x coated as well as AlO_x/acrylate topcoated film for both, oxygen and water vapour.

References

[1] C.A. Bishop, Roll-to-roll vacuum deposition of barrier coatings, Scrivener, Salem, 2010.

[2] The future of transparent barrier films to 2011, Pira International Ltd., Leatherhead, 2006.

[3] R.S.A. Kelly, 36th Annual Technical Conference Proceedings of the Society of Vacuum Coaters, 1993, p. 312.

[4] R.S.A. Kelly, 37th Annual Technical Conference Proceedings of the Society of Vacuum Coaters, 1994, p. 144.

[5] S. Schiller, M. Neumann, H. Morgner, N. Schiller, 37th Annual Technical Conference Proceedings of the Society of Vacuum Coaters, 1994, p. 203.

[6] S. Günther, S. Straach, N. Schiller, A.L. Quiceno, A.G. Contreras, R. Ludwig, G. Hoffmann, 52nd Annual Technical Conference Proceedings of the Society of Vacuum Coaters, 2009, p. 727.

[7] C.F. Struller, P.J. Kelly, N.J. Copeland, C.M. Liauw, J. Vac. Sci. Technol. A 30 (4) (2012) 041502.

[8] C.F. Struller, P.J. Kelly, N.J. Copeland, Surf. Coat. Technol., in press.

[9] A. Yializis, 38th Annual Technical Conference Proceedings of the Society of Vacuum Coaters, 1995, p. 95.

[10] J.D. Affinito, M.E. Gross, C.A. Coronado, G.L. Graff, I.N. Greenwell, P.M. Martin, Thin Solid Films 290–291 (1996) 63.

[11] J.D. Affinito, S. Eufinger, M.E. Gross, G.L. Graff, P.M. Martin, Thin Solid Films 308–309 (1997) 19.

[12] T. Miyamoto, K. Mizuno, N. Noguchi, T. Niijima, 44th Annual Technical Conference Proceedings of the Society of Vacuum Coaters, 2001, p. 166.

[13] G.L. Graff, R.E. Williford, P.E. Burrows, J. Appl. Phys. 96 (4) (2004) 1840.

[14] A. Yializis, M.G. Mikhael, R.E. Ellwanger, 43rd Annual Technical Conference Proceedings of the Society of Vacuum Coaters, 2000, p. 404.

[15] A.G. Erlat, B.M. Henry, C.R.M. Grovenor, A.G.D. Briggs, R.J. Chater, Y. Tsukahara, J. Phys. Chem. B 108 (3) (2004) 883.

[16] M. Hanika, H.-C. Langowski, U. Moosheimer, 45th Annual Technical Conference Proceedings of the Society of Vacuum Coaters, 2002, p. 519.

[17] E.H.H. Jamieson, A.H. Windle, J. Mater. Sci. 18 (1) (1983) 64.

[18] T.A. Beu, P.V. Mercea, Mater. Chem. Phys. 26 (3-4) (1990) 309.

[19] J.D. Affinito, D. Hilliard, 47th Annual Technical Conference Proceedings of the Society of Vacuum Coaters, 2004, p. 563.

[20] B.M. Henry, A.G. Erlat, C.R.M. Grovenor, C.-S. Deng, G.A.D. Briggs, T. Miyamoto, N. Noguchi, T. Niijima & Y. Tsukahara, 44th Annual Technical Conference Proceedings of the Society of Vacuum Coaters, 2001, p. 469.

[21] G. Aresta, J. Palmans, M.C.M. van de Sanden, M. Creatore, Microporous and Mesoporous Mater. 151 (2012) 434.

[22] Y.G. Tropsha, N.G. Harvey, J. Phys. Chem. B 101 (13) (1997) 2259.

[23] A.G. Erlat, R.J. Spontak, R.P. Clarke, T.C. Robinson, P.D. Haaland, Y. Tropsha, N.G. Harvey, E.A. Vogler, J. Phys. Chem. B 103 (29) (1999) 6047.

[24] A.P. Roberts, B.M. Henry, A.P. Sutton, C.R.M. Grovenor, G.A.D. Briggs, T. Miyamoto, M. Kano, Y. Tsukahara, M. Yanaka, J. Memb. Sci. 208 (1-2) (2002) 75.

[25] C.S. Deng, H.E. Assender, F. Dinelli, O.V. Kolosov, G.A.D. Briggs, T. Miyamoto, Y. Tsukahara, J. Polym. Sci. B Polym. Phys. 38 (23) (2000) 3151.

[26] S.-I. Hong, J.M. Krochta, J. Food. Eng. 77 (3) (2006) 739.

[27] M. Kurek, D. Klepac, M. Ščetar, K. Galić, S. Valić, Y. Liu, W. Yang, Polym. Bull. 67 (7) (2011) 1293.

[28] B.M. Henry, F. Dinelli, K.Y. Zhao, C.R.M. Grovenor, O.V. Kolosov, G.A.D. Briggs, A.P. Roberts, R.S. Kumar, R.P. Howson, Thin Solid Films 355-356 (1999) 500.

[29] B.M. Henry, D. Howells, J.A. Topping, H.E. Assender, C.R.M. Grovenor, L. Marras, 49th Annual Technical Conference Proceedings of the Society of Vacuum Coaters, 2006, p. 654.

[30] H.-C. Langowski, In: O.G. Piringer, A.L. Baner (Eds.), Plastic Packaging - Interactions with Food and Pharmaceuticals, Wiley-VCH, Weinheim, 2008, p. 297.

[31] O. Miesbauer, M. Schmidt, H.-C. Langowski, Vakuum in Forschung und Praxis 20 (2008) 32.

List of figure and table captions

Fig. 1: Arrhenius plots of ln(OTR), top, and ln(WVTR), bottom, as a function of 1/T for uncoated, AlO_x coated and acrylate topcoated BOPP.

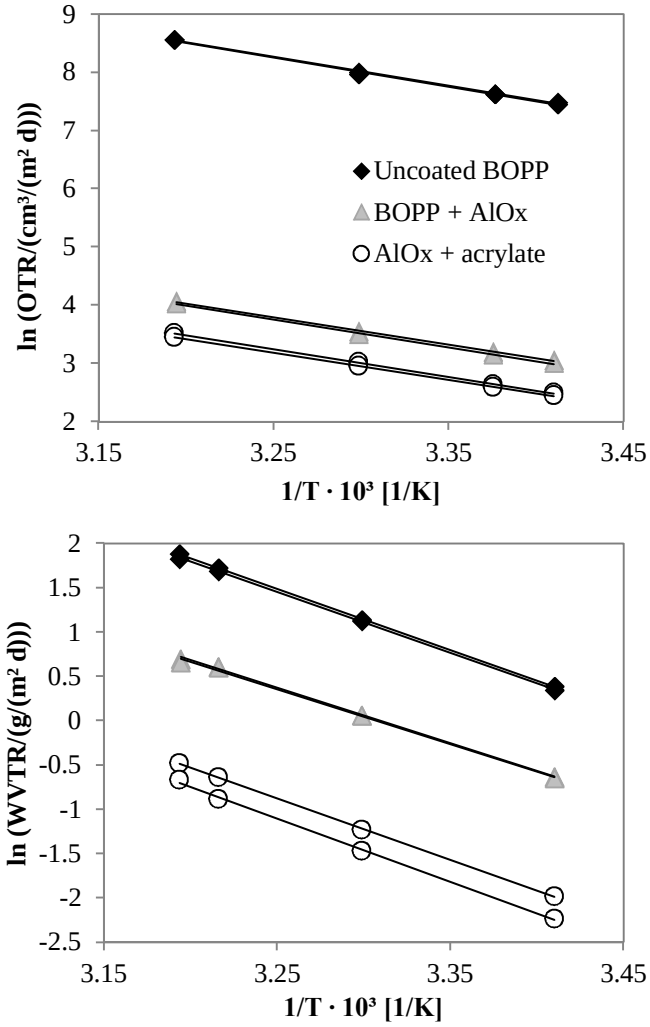

Fig. 2: Representative 5 x 5 µm² AFM scans of uncoated BOPP (top) and acrylate coated BOPP, undercoat, no AlO_x (bottom).

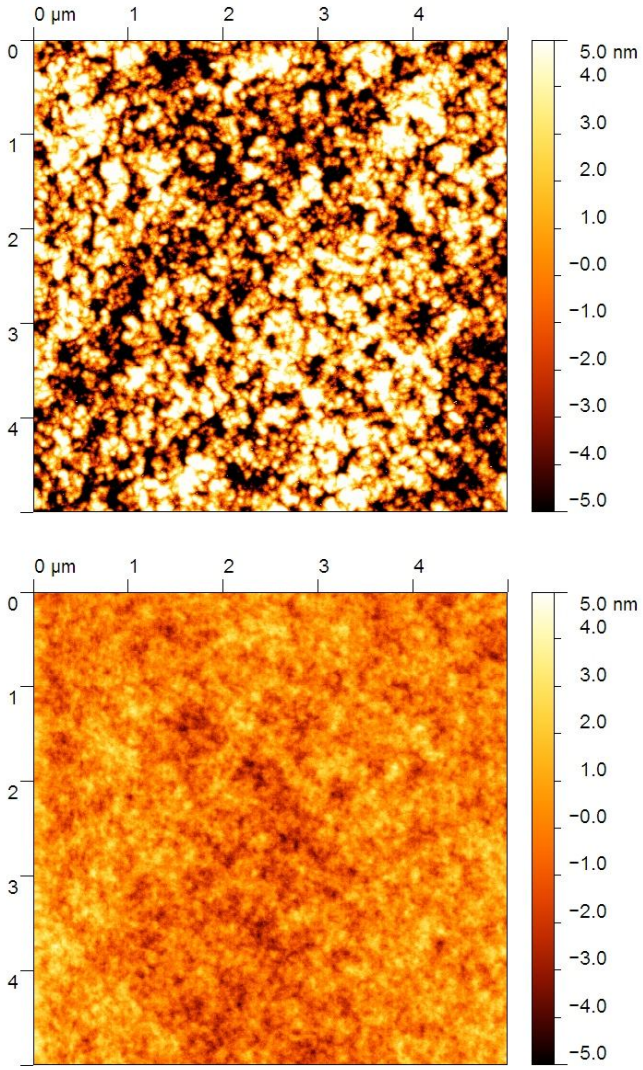

reproduced in color on the web and in black-and-white in print

Table I – Barrier performance of AlO_x coated BOPP in combination with acrylate top- and undercoats.

Description	**OTR**	**WVTR**
	$cm^3/(m^2\ d)$	**$g/(m^2\ d)$**
BOPP (uncoated)	≈ 2100	6 – 7
BOPP + *Acrylate undercoat*	1675.50 ± 129.40	6.59 ± 0.08
BOPP + *Acrylate undercoat* + AlO_x	15.83 ± 1.94	1.93 ± 0.21
BOPP + AlO_x	26.68 ± 3.07	4.73 ± 0.07
BOPP + AlO_x + *Acrylate topcoat*	13.65 ± 0.49	0.46 ± 0.07

Table II – Apparent activation energy E_A of oxygen and water vapour permeation through uncoated BOPP, AlO_x coated BOPP and acrylate topcoated AlO_x coated BOPP.

Description	**E_A (OTR)**	**E_A (WVTR)**
	kJ/mol	**kJ/mol**
BOPP (uncoated)	41.5 ± 0.3	57.3 ± 0.2
BOPP + AlO_x	39.4 ± 0.3	51.8 ± 0.4
BOPP + AlO_x + *Acrylate topcoat*	39.2 ± 0.7	58.6 ± 1.1

Table III – Barrier performance of AlO_x coated BOPP before and after adhesive lamination.

Description	**OTR**	**WVTR**
	$cm^3/(m^2\ d)$	**$g/(m^2\ d)$**
BOPP + AlO_x (before lamination)	48.62 ± 8.18	4.76 ± 0.35
BOPP + AlO_x + adhesive + BOPP (laminated)	11.92 ± 0.61	2.63 ± 0.17